Polymer 51 (2010) 2403–2409

Contents lists available at ScienceDirect

Polymer

journal homepage: www.elsevier.com/locate/polymer

Influence of zinc oxide nanoparticles on the crystallization behavior of electrospun poly(3-hydroxybutyrate-co-3-hydroxyvalerate) nanofibers

Wen Yu [a,b], Chin-Hung Lan [b], Shao-Jie Wang [a], Peng-Fei Fang [a], Yi-Ming Sun [b,c,d,*]

[a] Department of Physics Science and Technology, Wuhan University, Wuhan 430072, Hubei, China
[b] Department of Chemical Engineering and Materials Science, Yuan Ze University, Chung-Li 32003, Taiwan, ROC
[c] Graduate School of Biotechnology and Bioengineering, Yuan Ze University, Chung-Li 32003, Taiwan, ROC
[d] R&D Center for Membrane Technology, Chung Yuan University, Chung-Li, Taoyuan 32023, Taiwan, ROC

ARTICLE INFO

Article history:
Received 1 November 2009
Received in revised form
10 March 2010
Accepted 13 March 2010
Available online 27 March 2010

Keywords:
Electrospinning
Nanoparticles
Crystallization

ABSTRACT

Pure poly(3-hydroxybutyrate-co-3-hydroxyvalerate) (PHBV) and zinc oxide (ZnO)/PHBV composite nanofibers were fabricated by an electrospinning method. ZnO nanoparticles (NPs) with a diameter of about 10–20 nm were doped in the PHBV fibers and no dispersion agent was utilized. Both pure PHBV and composite electrospun fibers were smooth and uniform. ZnO NPs did not affect the basic crystalline structure of electrospun PHBV fibers. The well dispersion of NPs was attributed to the interaction of hydrogen bonds between −OH groups on the surface of ZnO and C=O groups in the PHBV. ZnO NPs were not nucleating or modifying agents but retarding agents for crystallization in the polymer matrix. The crystallinity and crystallization rate was lowered by adding ZnO NPs. The well dispersion of ZnO NPs in the electrospun nanofibers was confirmed by TEM characterization. A hypothesis was developed to interpret the influence of ZnO NPs on the crystalline behavior of electrospun PHBV fibers.

1. Introduction

Polyhydroxyalkanoates (PHAs) are a family of biological polyesters produced by microorganisms under unbalanced growth conditions [1]. By controlling the monomer composition of PHA, the physical properties of polymers can be regulated to a great extent. Compared with other biodegradable plastics from chemically synthesized polymers or starch-based biodegradable plastics, PHAs are the only 100% biodegradable and biosynthetic polymers [2]. This outstanding merit makes them attractive in many packaging, disposable items and biomedical applications.

The earliest discovered and most extensively studied PHA is poly (3-hydroxybutyrate) (PHB). However, the application of PHB is relatively limited due to its brittleness caused by its high crystallinity. Poly (3-hydroxybutyrate-co-3-hydroxyvalerate) (PHBV) copolymers with varying ratios of 3-hydroxyvalerate (HV) component are the most widely used member in PHAs. PHBV is more flexible and more readily processable than PHB mainly due to its lower crystallinity [3,4]. The crystalline structure, thermal properties, mechanical properties, degradation properties, etc., can be easily tuned by adjusting the ratio of HB (3-hydroxybutyrate) and HV in PHBV accordingly [5].

In order to further improve the properties of PHBV, incorporation of other functional additives into the polymer to form composites has received more and more attention. Organically modified montmorillonite (OMMT) was introduced into PHBV through polymer intercalation from solution [6]. With the incorporation of 3 wt.% OMMT, the tensile strength of the hybrid was about 32% higher than that of the original PHBV and the tensile modulus was also increased. Nanocomposites based on PHBV and multi-walled carbon nanotubes (MWNTs) were prepared using the similar method [7]. MWNTs were found to disperse uniformly in the matrix and their nucleating effect on PHBV made the composites more thermally stable than pure PHBV in nitrogen.

Notably, electrospinning, a simple and convenient process based on electrostatic force, has been largely developed in recent decades to fabricate ultrafine fibers with diameters typically in the range of several micros down to tens of nanometers [8,9]. Under the effect of the electrostatic force, a polymer solution jet from the spinning needle head is splayed and the polymer is solidified instantly due to the fast evaporation rate of the solvent in the electrospinning process. When nanomaterials are added and well dispersed in the polymer solution, they homogeneously are confined to the fiber matrix with no time to aggregate. The high electric fields can induce polarization and orientation of the nanomaterials, which

* Corresponding author at: Department of Chemical Engineering and Materials Science, Yuan Ze University, 135 Yuan Tung Road, Chung-Li 32003, Taiwan, ROC. Tel.: +886 3 4638800 2558; fax: +886 3 4559373.
E-mail address: cesunym@saturn.yzu.edu.tw (Y.-M. Sun).

0032-3861/$ – see front matter © 2010 Elsevier Ltd. All rights reserved.
doi:10.1016/j.polymer.2010.03.024

lead to the well embedding, dispersion and alignment of nanomaterials along the fiber matrices [10]. In order to increase the bioactivity of PHBV, hydroxyapatite (HA) and collagen were incorporated into PHBV to prepare nanofibers by electrospinning, respectively [11,12]. As an organosoluble salt (benzyl trialkylammonium chloride, BTEAC) was added to the PHBV electrospinning solution, the average fiber diameter decreased from 2.5 to 1.0 μm and the degradation of the fibers was accelerated [13].

The unusual and specific properties of inorganic nanomaterials have brought new direction in material science. There have been many efforts on the preparation of nanocomposites. However, the well dispersion of small size additives into polymer matrix is the primary problem to be resolved. Potential solutions such as ultrasonication [14], surface modifications [15], physical blending [16] and adding surfactants [17] have been reported. The issue remains a challenge to the preparation and usage of the nanocomposites. Moreover, the roles of nanomaterials during the fabrication of the nanocomposites and the interaction between organic and inorganic phases have not yet been intensively discussed.

Zinc oxide (ZnO) is not only a well-known semiconductor material for solar energy conversion [18], optoelectronic devices [19], piezoelectric generators [20], etc., but also an important additive in rubber and plastic industry for the purposes of antibacterial [21,22], antisepticizing [23], UV-shielding [24], deodorizing [25,26] and so on. It was found that particle size had an influence on the antibacterial activity: smaller ZnO particles had a better antibacterial activity due to larger surface area [27]. It is no doubt that the property of composite is greatly influenced by the degree of dispersion of NPs in the polymer matrix. In the few studies of ZnO NPs and polymer composites, ZnO NPs and poly (ethylene oxide) (PEO) [28] or polyethylene terephthalate (PET) [29] are connected by coupling agent and the former are regarded as a nucleating agent and can accelerate the crystallization of the polymers in the nanocomposites. Based on differential scanning calorimetric (DSC) data, it is found that ZnO NPs can speed up the crystallization rate and promote crystallization temperature of the polymer matrix.

Since PHBV is a kind of polyester without strong interactive functional groups, it is quite difficult to prepare well-dispersed composite of PHBV/inorganic materials. The puzzle lies in the stable combination of the two phases. To the best of our knowledge, there have been few reports or discussions concerning composite of PHBV/ZnO NPs and the interaction between them. In this study, we have prepared composite nanofibrous membranes with ZnO NPs and PHBV by the electrospinning method without any dispersion agent. The basic crystalline structure and the interaction between ZnO NPs and PHBV in the composite fibers are intensively studied. A primary model of the crystallization behavior of the electrospun composite fibers is proposed. It is hoped that this study will give a clue on the influence of the inorganic NPs on the crystallization behavior of the electrospun PHBV fibers.

2. Experimental

2.1. Materials

PHBV (with 5 wt.% of HV component, $M_w = 400{,}000$) was from Aldrich (St. Loius, MO, USA), chloroform was from Mallinckrodt (Hazelwood, MO, USA), dimethylformamide (DMF) was from Tedia (Fairfield, OH, USA), zinc acetate dehydrate ($Zn(CH_3COO)_2 \cdot 2H_2O$) was from Showa (Tokyo, Japan), lithium hydroxide monohydrate ($LiOH \cdot H_2O$) was from Tedia (Fairfield, OH, USA), absolute ethanol (200 proof) was from Echo (Taipei, Taiwan), and n-heptane was from Baker (Phillipsburg, NJ, USA).

2.2. Sample preparation

2.2.1. Synthesis of ZnO NPs

The ZnO NPs were self-made by a sol–gel process according to the reference [30]. Firstly, organometallic Zn precursor was prepared from $Zn(CH_3COO)_2 \cdot 2H_2O$ in ethanol by a 3 h reaction at 180 °C; then the ZnO clusters were formed by adding $LiOH \cdot H_2O$ in the precursor ethanol sol in an ice bath; finally, after crystal growth, the ZnO NPs were separated from the sol using heptane (as non-solvent for ethanol).

2.2.2. Preparation of electrospinning solution

PHBV in chloroform were stirred for at least 24 h to make sure that the molecular chains of the polymer are well entangled. Afterwards, DMF was added and then the solution was stirred for another 24 h. The final solution is composed of 4 wt.% PHBV in 90/10 chloroform/DMF co-solvent. Additional 1 wt.% ZnO NPs (based on PHBV) was added in the solution for the preparation of composite fibers. The doping concentration of ZnO NPs is 1 wt.% of the polymer and no higher concentration is utilized in this study. Firstly, high doping concentration will inevitable bring in aggregation problem. Moreover, it is reported that 1 wt.% ZnO doping can already result in an antibacterial efficiency of 99.7% while the efficiency is 99.996% at 2 wt.% [31]. Therefore, 1 wt.% ZnO doping concentration is considered effective for the antibacterial applications.

2.2.3. Electrospinning process

The electrospinning process for the preparation of pure PHBV and composite fiber membranes was similar to that in the previous report [32]. The applied voltage was 18 kV, the temperature was kept at 40 °C, the tip-to-collector distance was 25 cm, the feeding rate was 0.5 mL/h, and the collecting time was 6 h. Different from the reported one [32], a rotating mode was utilized and the rotating speed of the collector was 1200 rpm.

2.3. Characterization methods

The morphology of electrospun fibers was observed by scanning electron microscopy (SEM) (JEOL JSM-5600) equipped with an energy dispersive spectrometer (EDS). The average diameter of electrospun fibers was measured by analyzing the SEM image. First, five horizontal straight lines were drawn on a SEM picture. The diameters of all the fibers intersected with the straight lines were measured. Finally, these data were mathematically treated to obtain an average diameter of the electrospun fibers.

Crystalline diffraction patterns of ZnO NPs or nanofibers were determined by a wide angle X-ray diffractometer (WAXD, Shimadzu, XRD-600) operated at 40 kV and 30 mA, with Cu radiation ($\lambda = 0.1542$ nm). The scanning rate was 1°/min.

The micro-morphology was characterized with transmission electron microscope (TEM) (JEM2100, JEOL, Japan). The specimen of ZnO NPs for TEM observation was prepared by sonicating extreme small quantity of the NPs in the chloroform and a droplet was dispersed on a lacey carbon microgrid. The specimen of ZnO NPs/PHBV composite fibers for TEM observation was prepared by directly electrospinning the fibers on the microgrid. The fibers were collected by a random mode [31] with other parameters unchanged compared with the rotating mode (polymer concentration, temperature, applied voltage, feeding rate, collecting distance, etc.). The microgrid was placed in the center of the collecting area and the collecting time was 1 min. Composite PHBV fibers were imaged using a cryotransfer sample holder.

The chemical environments of the polymer molecules in the samples were tested by an attenuated total reflectance Fourier

transform infrared spectrometer (ATR-FTIR) (Perkin Elmer, USA). Each spectrum was collected by averaging 32 scans at a resolution of 4 cm^{-1}.

The thermal properties, such as heat capacity change (ΔC_p) at transition temperature, melting temperature (T_m), crystallization temperature (T_c), enthalpy of melting (ΔH_m), and enthalpy of crystallization (ΔH_c), of the nanofibrous membrane samples were determined by the differential scanning calorimeter (DSC) (Perkin Elmer DSC7, equipped with an intracooler). Samples were sealed in aluminum pans and scanned from −40 to 180 °C with a rate of 10 °C/min under a nitrogen atmosphere. The samples were kept at 180 °C for 5 min an then cooled to −40 °C with a cooling rate of 10 °C/min. Followed the cooling run, the samples were placed at −40 °C for 5 min and then heated again from −40 to 180 °C with a rate of 10 °C/min. According to the enthalpy of melting (ΔH_m), the relative crystallinity of the samples could be determined by:

$$X(\%) = \left(\frac{\Delta H_m}{\Delta H_{ref}}\right) \times 100\% \quad (1)$$

Where $\Delta H_{ref} = 138.7$ J/g. Here, the value of 138.7 J/g was estimated for the enthalpy of melting of the 100% crystallized HB fraction in the PHBV polymer (with 5 wt.% of HV component) [33].

3. Results and discussion

The properties of ZnO NPs are characterized first. From the sharp diffraction peaks in the XRD pattern (Fig. 1a), it can be deduced that ZnO NPs are well crystallized. By Scherrer formula [34], the crystallite size of the self-synthesized ZnO NPs is estimated about 11 nm from the strongest two peaks (<101> and <100 > directions). The NPs are characterized by TEM observation and the morphology is shown in Fig. 1b. ZnO NPs are of spherical shape and the apparent diameter of them is about 10–20 nm, which is consistent with that from the XRD results. Due to the annealing process, the NPs are well crystallized and clear lattices are observed in the TEM image. The crystalline direction is along hexagonal <0001> with the interplanar spacing of 0.261 nm. The insert in Fig. 1b is the selected area electron diffraction (SAED) pattern of the characterized area confirming the crystalline direction of the ZnO NPs.

Typical morphology of the electrospun PHBV nanofibers is shown in Fig. 2. It has been found that polymer concentration of 4 wt.% is an optimal concentration for the pure PHBV to produce smooth nanofibers with diameter of 300 ± 120 nm in our study. After adding 1 wt.% ZnO NPs in PHBV, the morphology of the obtained nanofibers does not change much except a smaller diameter (230 ± 70 nm) of the fibers in comparison with the pure PHBV fibers. Since ZnO is a typical semiconductor, during the electrospinning process, the polymer solution with ZnO NPs will have a larger charge capacity and then be driven by a stronger electric force along the fibers; therefore, smaller fiber diameter can be obtained in turn [13].

XRD results of the pure PHBV and composite fibrous membranes (Fig. 3) show that there is no new peak of PHBV after adding ZnO, indicating that ZnO does not significantly affect the crystalline structure of PHBV in the electrospinning process. Moreover, no peaks of ZnO are detected which may be due to the low doping concentration of ZnO NPs, which is just 1 wt.% and may be below the detection limit of the instrument. Calculated from the FWHM of the XRD data (peaks of <020> and <110>) by Scherrer formula [32], the crystallite size of PHBV decreases slightly after adding ZnO NPs (from 27 to 24 nm), implying that ZnO NPs may have a restrictive effect on the crystallite growth of PHBV.

In order to explore the role of ZnO NPs on the crystallization process of PHBV during the electrospinning process, ATR-FTIR is performed to detect the changes of chemical environment of the functional groups in PHBV after doping. The band at 1453 cm^{-1}, assigned to the scissoring vibration of CH_2 group, is taken as the reference peak since it is unconcerned with the conformation of PHBV. All the curves are normalized to be of same height (or area) at 1453 cm^{-1}.

The FTIR spectra of the carbonyl group (C═O) stretching band region (Fig. 4) has received much attention since the C═O bonds in PHBV are usually sensitive to crystalline phases. In this study, the curve fitting result reveals that there are only two peaks (1722 and 1731 cm^{-1}) in this region. The absorbance band at 1722 cm^{-1} is correlated to the antiparallel alignment of the 2_1 helix chain and assigned to the vibration of C═O in the crystalline state [35]. The band at 1731 cm^{-1} used to be related to the interphase between the lamellar crystallites and amorphous layers and generally named as rigid amorphous fraction (RAF) [36]. Recently, it is reported that this band should be related to intermediate state (between crystalline and amorphous states, or less ordered crystalline state). There have been several reports about the intermediate state, especially in the interpretation of the melt-crystallization process of PHB [37,38]. The band at 1740 cm^{-1} standing for the amorphous state [36] is not observed. The absence of amorphous state in this study may be due to the electrospinning process. The electric field has a strong elongation effect on the fibers by which the PHBV molecular chains tend to be oriented rather than randomly distributed as amorphous phase.

The weak peak at 1687 cm^{-1}, a crystalline sensitive band, is related to the crystal defect caused by the interaction of −OH end and C═O groups in PHBV [37]. It is found that the height (or area) of

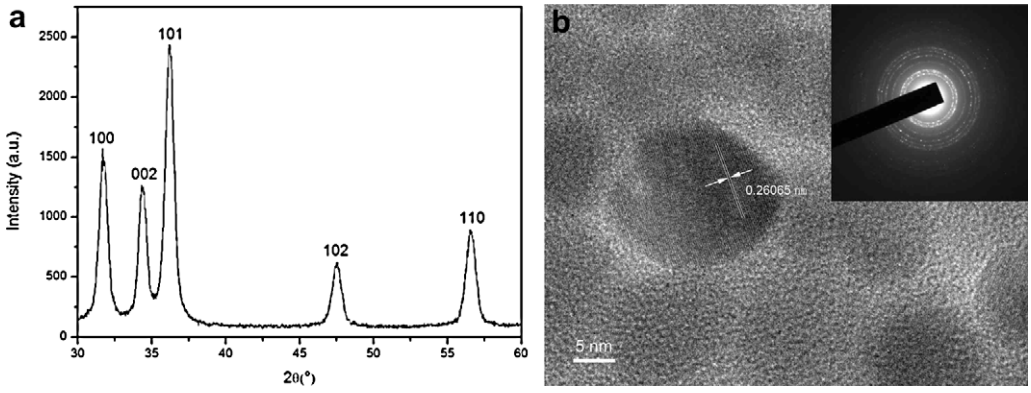

Fig. 1. (a) XRD pattern and (b) TEM image of the ZnO NPs.

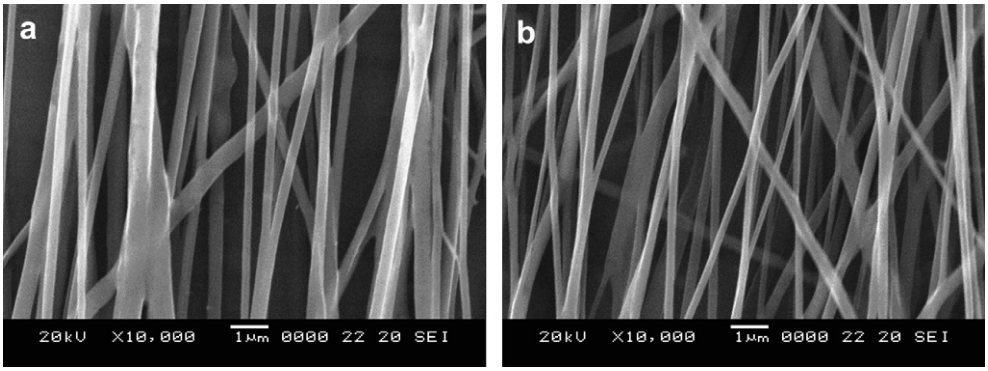

Fig. 2. SEM images of (a) the pure PHBV and (b) composite ZnO/PHBV nanofibrers.

the peak 1687 cm^{-1} after doping ZnO NPs becomes weaker (Table 1), i.e., less interaction of −OH end and C═O groups in PHBV. Since the peak at 1687 cm^{-1} locating on a strong background of the envelope of 1722 cm^{-1} band, we have removed the background in processing the data. Although the changes of those values are quite minimal and may be close to the resolution limit, the difference is still worth discussing. Usually, there are plenty oxygen vacancies on the surface of ZnO NPs and the −OH groups in the environment can be absorbed onto those vacancies [39]. Here in this experiment, ZnO NPs are synthesized by a sol–gel method using ethanol as solvent, therefore the surfaces of them are full of −OH groups which has been confirmed by FTIR test (data not shown here). These −OH groups can form hydrogen bonds with C═O groups and in turn decrease the chance of forming hydrogen bonds between −OH end and C═O group of PHBV. As a result, there is a decrease of the height (area) of the peak at 1687 cm^{-1} in the FTIR spectra after adding ZnO NPs.

In order to further study the influence of inorganic NPs on the crystallization behavior of electrospun PHBV nanofibers, DSC test is employed. The thermograms are illustrated in Fig. 5, and all the derived data are summarized in Table 2.

It is well accepted that C_p is usually related to the vibration of molecular chains and a drastic change of C_p in the heating process is a sign of the relaxation (glass transition) of the mobile molecular chains [40,41]. Here the transition temperatures are 61.3 °C (pure PHBV) and 57.0 °C (composite) (Fig. 5a) which are far above the common T_g of the raw PHBV (~0 °C). The common glass transition behavior is absent or very weak in both cases since the mobile molecular chains are not amorphous but intermediate phase (less ordered crystalline state). This is consistent with the former FTIR results (no peak at 1740 cm^{-1} has been observed or resolved by curve fitting). After adding ZnO NPs, ΔC_p increases from 0.135 to 0.174 J/g °C (Table 2). It indicates the amount of polymer at intermediate state increases. The crystallization of PHBV is partially retarded and the fraction of intermediate state increases.

It is well accepted that T_m is sensitive to lamella thickness [42,43]. However, in the first heating process of DSC, it is found that T_m does not significantly change before and after adding ZnO NPs. Thus it once again confirms that ZnO NPs do not influence the basic crystalline structure of electrospun PHBV fibers. The relative crystallinity decreases a bit after adding ZnO NPs (from 49.3 to 46.7%, calculated from ΔH_m according to eq. (1) [33]) implying that they act as a retarding agent for the crystallization in the electrospun PHBV fibers. In the cooling process (Fig. 5b), it is quite obvious that both T_c and ΔH_c decrease after adding ZnO NPs (Table 2). This follows what has been proposed: ZnO NPs retard the PHBV matrix from crystallization and slower the crystallization rate.

In the second heating process, dual melting peaks appear. The multiple melting peaks can arise either from compositional heterogeneity, multiple crystalline forms, or simply from melting–recrystallization–remelting (mrr) during the heating run [44–46]. Melting process (first heating) has destroyed the whole

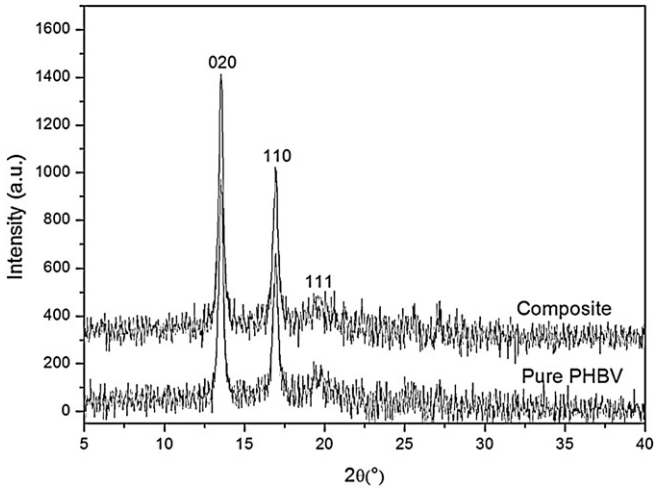

Fig. 3. XRD patterns of the pure PHBV and ZnO NPs/PHBV composite fibrous membranes (The curve of the composite membrane is moved upward for 500 intensity unit.).

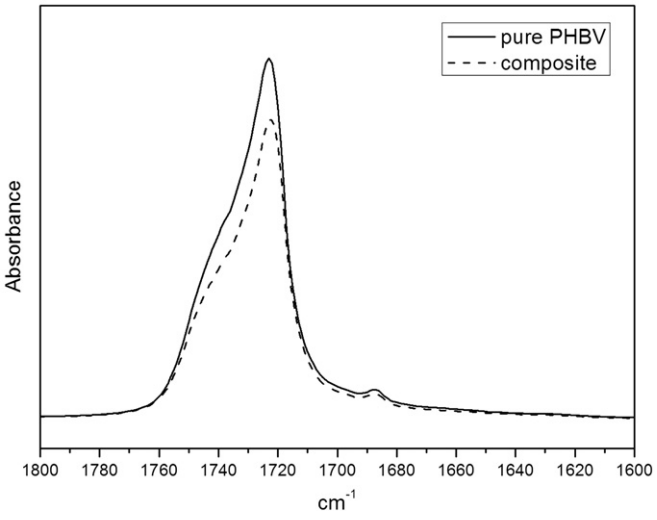

Fig. 4. FTIR spectra of the carbonyl group (C═O) stretching band region of pure PHBV and ZnO NPs/PHBV composite fibrous membranes. (Normalized to be of the same height at 1453 cm^{-1}).

Table 1
Chemical environment changes of 1687 cm^{-1} peak.

	Same height of 1453 cm^{-1} peak		Same area of 1453 cm^{-1} peak	
	Height (A)[a]	Area (A cm^{-1})	Height (A)	Area (A cm^{-1})
Pure PHBV	0.0042	0.0242	0.0028	0.0162
Composite	0.0039	0.0229	0.0027	0.0151

[a] Absorbance.

Table 2
Thermal properties of the electrospun PHBV or composite fibers.

	First heating			Cooling		Second heating	
	ΔC_p[a] (J/g °C)	T_m (°C)	ΔH_m (J/g)	T_c (°C)	ΔH_c (J/g)	T_m (°C)	ΔH_m (J/g)
Pure PHBV	0.135	168.2	68.3	58.5	−54.8	157.2	77.8
Composite	0.174	168.7	64.7	52.5	−47.1	143.1 and 159.2[b]	75.1

[a] Measured at the transition temperatures indicated in the Fig. 5a.
[b] Dual melting points shown in Fig. 5c.

crystalline structures and the thermal histories of the samples have been eliminated. The shoulder of the melting peak of pure PHBV in the second heating is ascribed to festinate cooling rate in the cooling process (10 °C/min). However, there are much more remarkable dual melting peaks for the composite (at 143.1 °C and 159.2 °C, respectively). Hence it is no doubt that, the first melting peak stands for the melting of secondary crystallites. Hindered by NPs, there is much more secondary crystallization in the composite than the pure one during the cooling run or the earlier stage in the second heating run. The secondary crystalline phase melts at a lower T_m, crystallizes, and remelts again at a higher temperature during the second heating. After the first heating and cooling processes, the samples are no longer the same as the original electrospun nanofibrous membranes. They behave like ordinary PHBV or ZnO NPs/PHBV composites and the common T_gs around 0 °C can be observed. A small crystallization peak around 45 °C is found for the composite. It further demonstrates the retarding effect of ZnO NPs in the melt crystallization during the cooling run.

It is widely accepted that the crystallinity of the polymer matrix will increase through adding nanomaterials which serve as nucleating agent [47–49]. However, here in this study, it is quite different from the general cases that the crystallinity of the electrospun PHBV fibers does not increase but decreases after adding ZnO NPs. This unusual phenomenon is mainly ascribed to two factors: the special crystalline structure of PHBV and the interaction between the two components.

In general, the crystalline region of a polymer is composed of lamellar stacks where there is alternatively stacking of crystalline and amorphous phases (long period) [50]. According to the XRD and SAXS results, the size of the lamellar stacks (crystallite size) decreases slightly (Fig. 3) but the thickness of the repeating lamellar/intermediate (complete amorphous phase is absent according to the FTIR result) layers do not change before and after adding ZnO NPs (from SAXS, data not shown). Therefore, the crystalline behavior of electrospun PHBV fiber is illustrated in Fig. 6a. PHBV α-helix regularly folds as crystalline layer and the space between the crystalline layers is intermediate phase. These repeating layers form stacking structure in the fibers. Based on the strong diffraction peaks of <020> and <110> directions in the XRD pattern of the electrospun fibers, it can be deduced that the nanofibers and the α-helixes are parallel to the c axis (<001> direction) and the lamellae are almost perpendicular to the fiber direction.

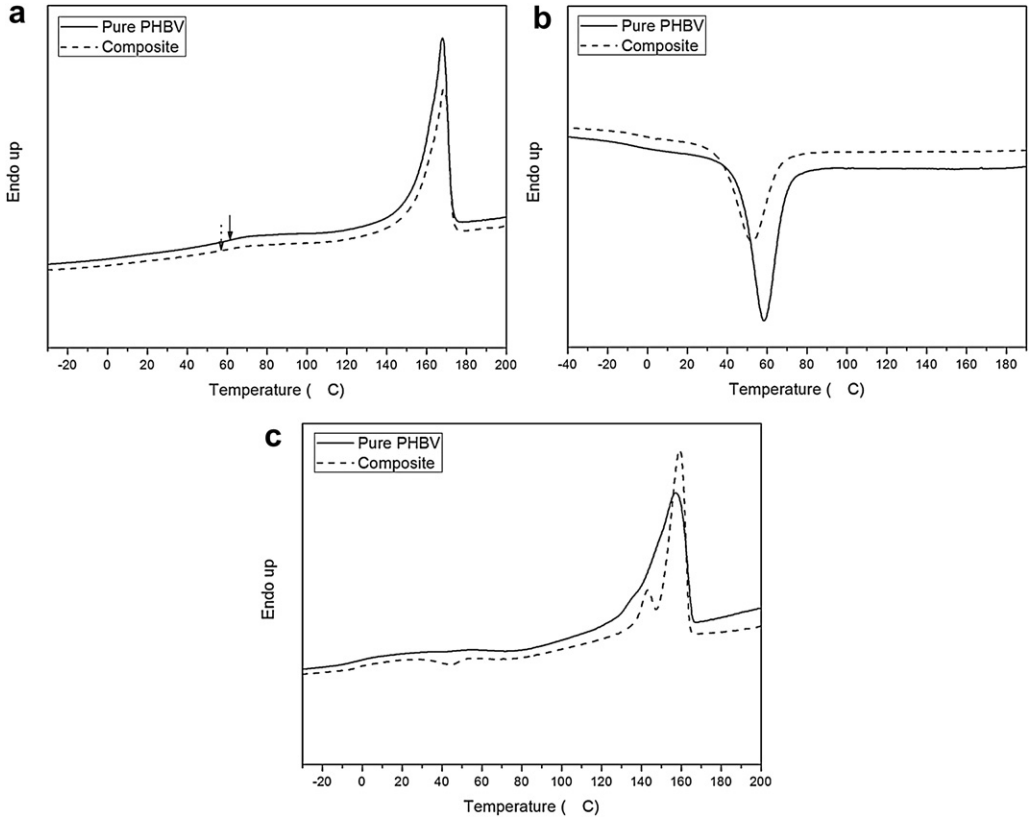

Fig. 5. DSC thermograms of the pure PHBV and composite fibrous membranes. (a) first heating, (b) cooling, and (c) second heating.

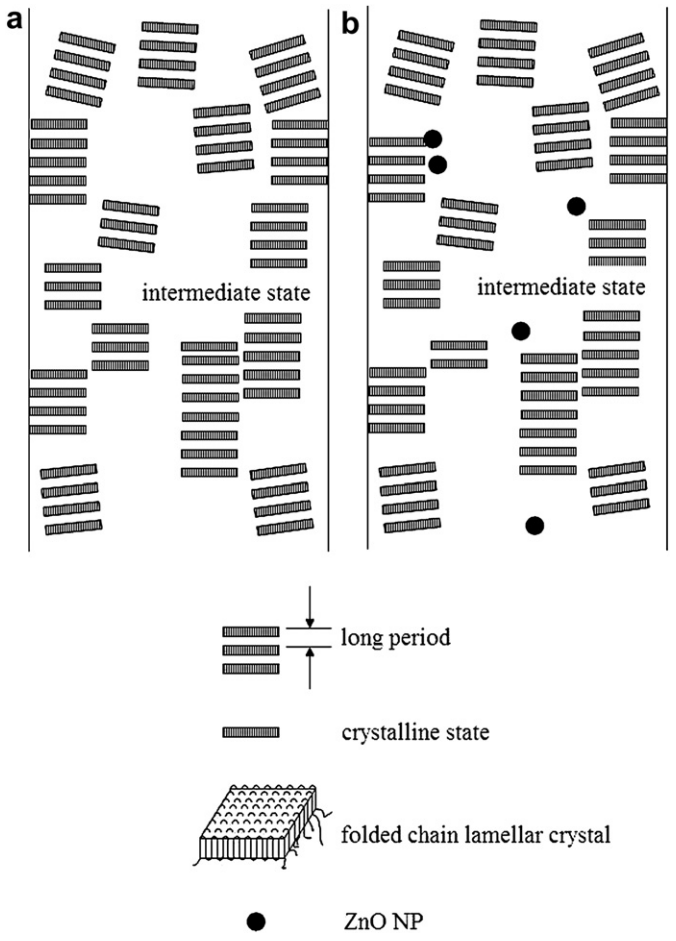

Fig. 6. Sketches of the (a) pure PHBV and (b) composite ZnO NPs/PHBV fiber.

Moreover, it has been reported that in the case of the electrospun nanofibers of PET containing TiO_2 NPs [51], the two components can form network which hinders the crystallization of PET chains. There is a similar interaction in this study: hydrogen bonds are formed between PHBV and ZnO NPs. The crystallinity of the electrospun fiber decreases after adding ZnO NPs. Based on the experimental evidences discussed earlier, a hypothesis is set up to interpret the influence of ZnO NPs on the crystalline behavior of PHBV in the electrospinning process. A schematic description of this influence is demonstrated in Fig. 6b. Hydrogen bonds are formed between −OH groups on ZnO NPs and C═O in PHBV. In the crystallization process, ZnO NPs disturb the regularity of PHBV molecular chains which in turn decreases the PHBV crystallinity of the electrospun composite fibers and the PHBV crystallite size of the lamellae in the fibers. The mobility of random macromolecular chains is lower than the original amorphous phase and addressed as intermediate phase. The amount of intermediate phase in the PHBV fibers increases after adding ZnO NPs.

TEM images of the composite fibers are presented in Fig. 7. Dispersion of ZnO NPs in the electrospun fibers is quite well although they are retarding agent for the crystallization of the polymer matrix. There is no serious agglomeration of ZnO NPs in the polymer. It is worth mentioned that ZnO NPs do not distribute evenly in every part of the fibers. In another words, they prefer certain regions to somewhere else. Based on the hypothesis discussed above, it can be deduced that the location with more ZnO NPs should be intermediate phase where there are more irregular PHBV molecular chains. As a consequence, there is much less possibility for NPs to distribute in the well crystalline state. However, further rigorous characterizations are still needed, such as a TEM test of the cross-section of the electrospun composite fibers with dyeing treatment so as to clearly distinguish different crystalline phases.

4. Conclusions

Pure PHBV and ZnO NPs/PHBV composite nanofibers are fabricated by the electrospinning process. To some extent, the doping of the ZnO NPs decreases the diameter of the electrospun fibers. The basic crystalline structure of the PHBV is not influenced by the NPs. However, the interaction of hydrogen bonds between ZnO NPs and PHBV hinders the crystallization of the latter. A schematic morphological model of the electrospun PHBV composite fibers is given accordingly. The present study sheds a light on the influence of the inorganic nanoparticles with hydroxyl groups on the crystallization behavior of electrospun PHBV nanofibers. Even without the use of a dispersion agent, the compatibility of ZnO NPs with other carbonyl group containing polymers, such as polyacrylates, polymethacrylates, and polyesters, could be expected from the finding of this study. The effect of hydrogen-bonding interaction between the hydrophilic surface of inorganic NPs and the polar groups of the polymers should be carefully examined although the polymers themselves are considered hydrophobic.

Acknowledgments

This work was supported by the National Science Council of the Republic of China through the grants of NSC97-2221-E-155-003-MY2 and NSC98-2622-E-155-003-CC2. W. Yu would like to thank Yuan Ze University for providing the exchange student scholarship during the period of this study.

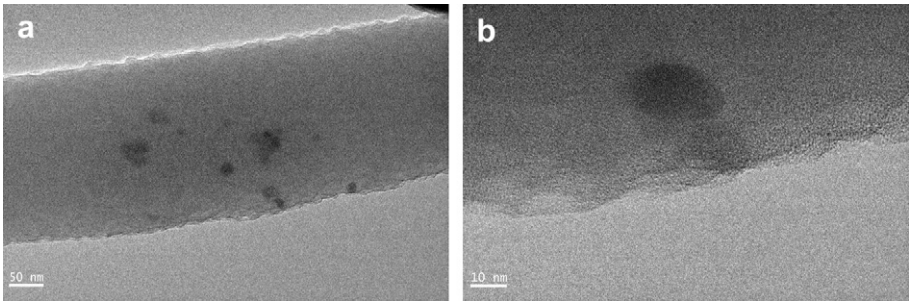

Fig. 7. TEM images of the composite ZnO NPs/PHBV fibers.

References

[1] Doi Y, Steinbüchel A. Biopolymers. Weinheim, Germany: Wiley-VCH; 2002.
[2] Khanna S, Srivastava AK. Process Biochem 2005;40:607.
[3] Mitomo H, Barham PJ, Keller A. Polym J 1987;19:1241.
[4] Gassner F, Owen AJ. Polym Int 1996;39:215.
[5] Byrom D. Polyhydroxyalkanoates. In: Mobley DP, editor. Plastics from microbes: microbial synthesis of polymers and polymer precursor. Munich: Hanser; 1994.
[6] Chen GX, Hao GJ, Guo TY, Song MD, Zhang BH. J Mater Sci Lett 2002;21:1587.
[7] Lai MF, Li J, Yang J, Liu JJ, Tong X, Cheng HM. Polym Int 2004;53:1479.
[8] Huang ZM, Zhang YZ, Kotaki M, Ramakrishna S. Compos Sci Technol 2003;63:2223.
[9] Li D, Xia YN. Adv Mater 2004;16:1151.
[10] Yu G, Li XH, Cai XJ, Cui WG, Zhou SB, Weng J. Acta Mater 2008;56:5775.
[11] Ito Y, Hasuda H, Kamitakahara M, Ohtsuki C, Tanihara M, Kang I, et al. J Biosci Bioeng 2005;100:43.
[12] Meng W, Kim S, Yuan J, Kim JC, Kwon OH, Kawazoe N, et al. Biomater Sci Polym Ed 2007;18:81.
[13] Choi JS, Lee SW, Jeong L, Bae S, Min BC, Youk JH, et al. Int J Biol Macromol 2004;34:249.
[14] Misra AK, Nazhat SN, Valappil SP, Torbati MM, Wood RJK, Roy I, et al. Biomacromolecules 2007;8:2112.
[15] Nichols HL, Zhang N, Zhang J, Shi D, Bhaduri S, Wen XJ. Biomed Mater Res 2007;82A:373.
[16] Coskun S, Korkusuz F, Hasirci VJ. Biomater Sci Polym 2005;16:1485.
[17] Kim HW. J Biomed Mater Res 2007;83A:169.
[18] Rensmo H, Keis K, Lindstrom H, Solbrand A, Hagfeldt A, Lindquist SE, et al. J Phys Chem B 1997;101:2598.
[19] Zhang XT, Liu YC, Zhang LG, Zhang JY, Lu YM, Shen DZ, et al. J Appl Phys 2002;92:3293.
[20] Zhou J, Fei P, Gao YF, Gu YD, Liu J, Bao G, et al. Nano Lett 2008;8:2725.
[21] Xu T, Xie CS. Prog Org Coat 2003;46:297.
[22] Zhang LL, Jiang YH, Ding YL, Povey M, York DJ. Nanopart Res 2007;9:479.
[23] Amalric L, Guillard C, Pichat P. Res Chem Intermed 1994;20:579.
[24] Tu Y, Zhou L, Jin YZ, Gao C, Ye ZZ, Yang YF, et al. J Mater Chem 2010;20:1594.
[25] Saito M. J Ind Text 1993;23:150.
[26] Kim HT, Jun KW, Kim SM, Potdar HS, Yoon YS. Energy Fuels 2006;20:2170.
[27] Yamamoto O. Int J Inorg Mater 2001;3:643.
[28] Xiong HM, Zhao X, Chen JS. J Phys Chem B 2001;105:10169.
[29] He JQ, Shao W, Zhang L, Deng C, Li CZ. J Appl Polym Sci 2009;114:1303.
[30] Spanhel L, Anderson MA. J Am Chem Soc 1991;113:2826.
[31] Li YF, Wang BH, Huang WX, Tu MJ. New Chem Mater 2002;30:44 [In Chinese].
[32] Cheng ML, Lin CC, Su HL, Chen PY, Sun YM. Polymer 2008;49:546.
[33] Cheng ML, Sun YM. Polymer 2009;50:5298.
[34] Patterson AL. Phys Rev 1939;56:978.
[35] Yokouchi M, Chatani Y, Tadokoro H, Teranishi K, Tani H. Polymer 1973;14:267.
[36] Yoshie N, Oike Y, Kasuya K, Doi Y, Inoue Y. Biomacromolecules 2002;3:1320.
[37] Zhang JM, Sato H, Noda I, Ozaki Y. Macromolecules 2005;38:4274.
[38] Padermshoke A, Katsumoto Y, Sato H, Ekgasit S, Noda I, Ozaki Y. Spectrochim Acta Part A 2005;61:541.
[39] Daneshvar N, Salari D, Khataee AR. J Photochem Photobiol A 2004;162:317.
[40] Birge NO, Nagel SR. Phys Rev Lett 1985;54:2674.
[41] Gobrecht H, Hamann K, Willers GJ. Phys E Sci Instrum 1971;4:21.
[42] Cser F. J Appl Polym Sci 2001;80:358.
[43] Dlugosz J, Fraser GV, Grubb D, Keller A, Odell JA, Goggin PL. Polymer 1976;17:471.
[44] Chen C, Cheung MK, Yu PHF. Polym Int 2005;54:1055.
[45] Androsch R. Polymer 2008;49:4673.
[46] Hong PD, Chuang WT, Yeh WJ, Lin TL. Polymer 2002;43:6879.
[47] Tang JG, Wang Y, Liu HY, Belfiore LA. Polymer 2004;45:2081.
[48] Kim G, Wutzler A, Radusch H, Michler GH, Simon P, Sperling RA, et al. Chem Mater 2005;17:4949.
[49] Cai YB, Li Q, Wei QF, Wu YB, Song L, Hu YJ. Mater Sci 2008;43:6132.
[50] Fujiwara YJ. Appl Polym Sci 1960;4:10.
[51] Meng XF, Luo N, Cao SL, Zhang SM, Yang MS, Hu X. Mater Lett 2009;63:1401.